



Noise Reduction Potential of Large, Over-the-Wing Mounted, Advanced Turbofan Engines

Jeffrey J. Berton
Glenn Research Center, Cleveland, Ohio

The NASA STI Program Office . . . in Profile

Since its founding, NASA has been dedicated to the advancement of aeronautics and space science. The NASA Scientific and Technical Information (STI) Program Office plays a key part in helping NASA maintain this important role.

The NASA STI Program Office is operated by Langley Research Center, the Lead Center for NASA's scientific and technical information. The NASA STI Program Office provides access to the NASA STI Database, the largest collection of aeronautical and space science STI in the world. The Program Office is also NASA's institutional mechanism for disseminating the results of its research and development activities. These results are published by NASA in the NASA STI Report Series, which includes the following report types:

- **TECHNICAL PUBLICATION.** Reports of completed research or a major significant phase of research that present the results of NASA programs and include extensive data or theoretical analysis. Includes compilations of significant scientific and technical data and information deemed to be of continuing reference value. NASA's counterpart of peer-reviewed formal professional papers but has less stringent limitations on manuscript length and extent of graphic presentations.
- **TECHNICAL MEMORANDUM.** Scientific and technical findings that are preliminary or of specialized interest, e.g., quick release reports, working papers, and bibliographies that contain minimal annotation. Does not contain extensive analysis.
- **CONTRACTOR REPORT.** Scientific and technical findings by NASA-sponsored contractors and grantees.

- **CONFERENCE PUBLICATION.** Collected papers from scientific and technical conferences, symposia, seminars, or other meetings sponsored or cosponsored by NASA.
- **SPECIAL PUBLICATION.** Scientific, technical, or historical information from NASA programs, projects, and missions, often concerned with subjects having substantial public interest.
- **TECHNICAL TRANSLATION.** English-language translations of foreign scientific and technical material pertinent to NASA's mission.

Specialized services that complement the STI Program Office's diverse offerings include creating custom thesauri, building customized data bases, organizing and publishing research results . . . even providing videos.

For more information about the NASA STI Program Office, see the following:

- Access the NASA STI Program Home Page at <http://www.sti.nasa.gov>
- E-mail your question via the Internet to help@sti.nasa.gov
- Fax your question to the NASA Access Help Desk at (301) 621-0134
- Telephone the NASA Access Help Desk at (301) 621-0390
- Write to:
NASA Access Help Desk
NASA Center for Aerospace Information
7121 Standard Drive
Hanover, MD 21076



Noise Reduction Potential of Large, Over-the-Wing Mounted, Advanced Turbofan Engines

Jeffrey J. Berton
Glenn Research Center, Cleveland, Ohio

Prepared for the
14th International Symposium on Air Breathing Engines
sponsored by the International Society for Air Breathing Engines
Florence, Italy, September 5–10, 1999

National Aeronautics and
Space Administration

Glenn Research Center

Acknowledgments

Thanks to David Elliott of NASA Glenn for providing the experimental Low Noise Fan data used in this study.

Trade names or manufacturers' names are used in this report for identification only. This usage does not constitute an official endorsement, either expressed or implied, by the National Aeronautics and Space Administration.

Available from

NASA Center for Aerospace Information
7121 Standard Drive
Hanover, MD 21076
Price Code: A03

National Technical Information Service
5285 Port Royal Road
Springfield, VA 22100
Price Code: A03

Noise Reduction Potential of Large, Over-the-Wing Mounted, Advanced Turbofan Engines

Jeffrey J. Berton*

National Aeronautics and Space Administration
Glenn Research Center
Cleveland, Ohio

As we look to the future, increasingly stringent civilian aviation noise regulations will require the design and manufacture of extremely quiet commercial aircraft. Indeed, the noise goal for NASA's Aeronautics Enterprise calls for technologies that will help to provide a 20 EPNdB reduction relative to today's levels by the year 2022. Further, the large fan diameters of modern, increasingly higher bypass ratio engines pose a significant packaging and aircraft installation challenge. One design approach that addresses both of these challenges is to mount the engines above the wing. In addition to allowing the performance trend towards large, ultra high bypass ratio cycles to continue, this over-the-wing design is believed to offer noise shielding benefits to observers on the ground. This paper describes the analytical certification noise predictions of a notional, long haul, commercial quadjet transport with advanced, high bypass engines mounted above the wing.

Introduction

The overall noise signature of advanced turbofan engines with highly loaded, wide chord fan blades will be dominated by fan discharge noise. Modern, high pressure cores and high bypass ratio cycles extract significant energy from the core air flow, which tends to reduce primary jet noise. This contrasts with older technology engines, where jet noise is prominent and where fan inlet noise is at least as high as fan discharge noise. Previous investigations of mounting older technology engines above the wing have shown limited noise reduction benefits. Bloomer (Ref. 1), for example, experimentally demonstrated wing shielding reductions of less than 3 EPNdB because the wing chord was not sufficiently large to shield both ends of the engine. Jet noise is particularly difficult to shield efficiently because it is often a distributed source downstream of the wing. It is anticipated that, with fan discharge noise dominating modern turbofans and with jet noise becoming less prominent, wing shielding will be much more effective. Mounting the engines above the wing also allows designers to install increasingly larger diameter engines more easily and allows the performance trend towards ultra high bypass ratio cycles to continue.

Other benefits of an over-the-wing design include shorter, lighter landing gear, and interference installation drags as low as those encountered in current under-the-wing configurations. An increase in lift may be possible via the Coanda surface effect. Unfortunately, engine maintenance would be more complex, new servicing rigs and lifts would be required, and cabin noise may increase. Such a configuration would also require a shift away from current, traditional, airframe design philosophies. Engine support structures, wing boxes, and even empennage would need to be designed much differently for over-the-wing installations. The

higher center of gravity may cause stability concerns. These issues all need to be carefully considered. This study, however, focuses simply on quantifying the benefit of noise reduction caused by the shielding effect of advanced turbofan engines mounted above the wing.

The aircraft considered is a notional, large, long haul quad with high bypass turbofan engines in the 55000-pound thrust class. Entry into service is approximately 2020. A large quad is chosen because, even under current regulations, such aircraft sometime experience difficulty complying with certification noise requirements with a substantial margin. This is especially true at the approach measurement location. With its long chord lengths, a large airplane would take greatest advantage of any noise shielding benefit.

A thermodynamic cycle analysis is performed on the engine. Thrust, spool speeds, jet properties, and other thermodynamic and aeromechanical data are predicted so that jet and core noise can be properly calculated. Fan inlet and discharge source noise are predicted across all throttle settings using actual experimental acoustic data measured from Pratt & Whitney Advanced Ducted Propulsor rig tests. The apparent attenuation of the fan and core source noise due to wing shielding is predicted using a classic partial barrier diffraction analysis. Noise levels appropriate for U.S. Federal Aviation Regulation certification are predicted for both conventional and over-the-wing mounted configurations.

Method of Analysis

Fan noise is predicted using the acoustic test results of Pratt & Whitney's Low Noise Fan Number 1 (Ref. 2). The fan is a 22-inch diameter scale model with 18 blades and 45 vanes. The inlet, interstage, and aft

*Aerospace Engineer, Propulsion Systems Analysis Office.

portions of the duct are lined with a two degree of freedom acoustic treatment material. The test facility is the NASA Glenn 9×15 Low Speed Wind Tunnel (Figure 1) where an air turbine drive powers the test article. The acoustic data are collected using a 48-position traversing microphone and three stationary microphones at yaw angles ranging from 27 to 160 degrees from the inlet axis. The data are corrected for electronic phenomena such as microphone response, cable response, and filter response as well as atmospheric attenuation. The tunnel is anechoic down to 250 Hz and is operated at a freestream Mach number of 0.1. The physical, geometric yaw angles are converted to emission angles to correct for the convective flow of the tunnel. The fan is designed for a full scale diameter of 130 inches, a design point pressure ratio of 1.28, a bypass ratio of 13.5, and a tip speed of only 850 ft/s.

Narrow band data taken at a constant bandwidth of 59 Hz is the basis of the fan noise modeling process. Acoustic pressure level data at each of the 51 microphone locations are scaled to full size in amplitude using the area scaling factor multiplier, and are shifted in frequency by the linear scale factor. The data are then brought to static conditions by assuming each sound pressure level scales with fan power and specific work, and normalizing that product by the appropriate convective amplification factor. The convective amplification factor is a function of the yaw angle of the data being transformed, the tunnel Mach number, and an assumed fourth-power exponent on the Doppler shift term.

The measured sound pressure levels are not used directly in this analysis. Instead, a curve-fitting approach is used so that the noise levels can be more accurately extrapolated to yaw angles close to the engine axis. This is important for many aircraft-observer orientations where fan noise still contributes to the certification noise calculation, but where the yaw angles needed are beyond those measured in the test. The noise data are therefore smoothed using immediately adjacent values in both frequency and yaw angle space. This process is shown in Figure 2 for a yaw angle of 130 degrees and the maximum takeoff rated fan speed. Tunnel background noise is also removed during this step. The broadband noise is approximated by a single mode of propagation in frequency f and is modeled as an exponential of the form $a_1[\ln(f/f_p)]^2 + a_2$, where f_p is the frequency of the peak broadband noise level, and the a_i are best fit constants. The fundamental and harmonic interaction tones do not contribute to the broadband curve fit and are modeled separately. The noise spectra are then converted to preferred, 1/3rd octave, proportional band spectra as shown in the figure. Each tone is placed on the nearest center frequency so

that their levels are not reduced in the transformation. A change in each of the spectra may not be observed unless the Doppler shift is large enough to shift the acoustic energy into an adjacent bin. Disappearance of the fundamental tone into the broadband noise at many angles attests to good measures of flight cleanup and liner performance.

Inlet and discharge components of the fan noise are separated using data taken in the presence of an acoustic barrier wall that effectively removes the influence of the discharge noise at high yaw angles. The static, free field, tone-weighted perceived noise levels at fixed radii are shown in Figure 3 for the fan at maximum rated takeoff speed. The dominance of the discharge noise is clearly seen. This is compared in the figure with equivalent static data of an older technology CF6-80C2 fan (Ref. 3), which is dominated by inlet noise. It is worth mentioning that the CF6 data shown is at a reduced power setting, and the multiple pure tones that radiate out of the inlet at higher speeds only serve to further increase the CF6 inlet noise. With nearly all of the noise of the current fan concentrated at the exit plane, wing shielding is expected to be very effective.

The free field, tone-weighted perceived noise levels at fixed radii for each of the power settings is shown in Figure 4. The influence of convective amplification at 200 knots airspeed is also shown.

The diffraction analysis used in this study is based on asymptotic results of optical diffraction theory, originally proposed by Maekawa (Ref. 4) and reproduced in many foundational acoustic textbooks. The engine and wing arrangement is approximated by an incoherently radiating fan noise point source on the engine centerline situated above a barrier wing. The analytic treatment of diffraction effects in this manner is common in aeroacoustic applications such as these (e.g., Ref. 5). Spectral barrier attenuation levels are calculated and applied separately to fan inlet and discharge sources as the aircraft flies past ground level certification observers. The shadow zone barrier attenuation is

$$L_B = 20 \log_{10} \left(\sqrt{2\pi|N|} / \tanh \sqrt{2\pi|N|} \right) + 5,$$

where N is the wavelength-dependent Fresnel number whose characteristic length is the difference between the shortest path around the barrier between the source and the observer and the source-observer distance directly through the barrier. For observers in the bright zone ($N < -0.192$), the attenuation is neglected, and for observers in the transition zone ($-0.192 < N < 0$), it is appropriate to replace the hyperbolic tangent with the

trigonometric tangent. Although the above formulation is intended for semi-infinite barriers, Maekawa suggests that superposition may be used for barriers of finite length and width. In this study, the attenuation is calculated over both leading and trailing edges of the wing and the resulting fields are summed. The geometry of the engine and airframe layout used in this study is shown in Figure 5 and Table 1. Note that the engines are assumed to be mounted forward of the wing's leading edge in typical fashion to help delay the onset of flutter. Inlet and discharge barrier attenuation levels are shown in Figures 6 and 7, respectively.

Actual barrier attenuation is often less than that predicted by theory or measured in an anechoic facility. Distributed sources do not attenuate as well as point sources. Although acoustically compact, the fan in this study is not an ideal point source. Temperature and wind stratification and atmospheric turbulence limits the barrier attenuation as well. Wing tip vortices are also known to cause additional refraction effects in tri-jets (Ref. 6) and may affect noise from over-the-wing mounted engines. Also, the refraction of sound in the trailing wake of the wing is not predicted by theory and will cause additional propagation into the shadow zone. Experimental tests conducted by Hellstrom (Ref. 7), however, generally show good agreement between measured data and simplified analytical diffraction predictions such as these. In any case, a maximum, practical, typical attenuation limit of 24 dB is used in this study, and it is emphasized that the diffraction analysis performed here is only a first approximation.

Jet noise is treated as a distributed source several diameters downstream of the installation and is not subject to diffraction calculations. Pratt & Whitney was tasked with experimentally measuring the jet noise of a coannular nozzle designed to operate in an engine with the same Low Noise Fan used here. In that study, Low (Ref. 8) compared the experimental acoustic results from his scale model nozzle with the SAE prediction (Ref. 9) and found the method to overpredict the jet noise by 5 to 6 dB across all operating conditions. This is not unexpected, since the secondary-to-primary area ratio of the test nozzle (7.1) exceeds the range of the SAE database (3.5). The Stone jet noise model (Ref. 10), however, is based on area ratios as high as 43.5. The predictions of the two methods are compared to Low's data in Figure 8 for the highest nozzle pressure ratio test. The data are scaled to full size and are shown at a fixed, 150 foot radius. Although the Stone model performs somewhat better, it also does not reliably predict the expected levels. A generalized analytic model is preferred over simply using Low's test data, since the jet properties predicted by cycle calculations at various certification conditions may differ from those used in

the tests. Therefore, the peak level predictions in the Stone method are modified to match those measured by Low. Stone's forward flight effect model is also replaced by the method suggested by Low based on his freejet data. This modified Stone method is used in all calculations performed here. No noise installation effects are predicted for cases where the engines are mounted below the wing.

Core noise is calculated using the method developed by Emmerling (Ref. 11). For over-the-wing calculations, the core source noise is subjected to the same barrier attenuation as the fan discharge noise. Airframe noise is calculated using the method developed by Fink (Ref. 12). To be consistent with expected airframe noise levels of 2020, 4 dB is subtracted from all airframe source noise calculations. This is consistent with the demonstrated noise reduction element goals of NASA's Advanced Subsonic Technology Program (See, e.g., Ref. 13). Turbine source noise is not calculated in this study because the existing NASA methods are known to be significantly inaccurate in both absolute level and in spectral distribution (Ref. 3). Thankfully, turbine noise is not likely to dominate (Ref. 13), and its omission from this study may not be a bad assumption. Noise propagation effects considered include spherical spreading, Doppler shift and amplification, atmospheric attenuation (Ref. 14), ground reflections (Ref. 15) based on data for grass-covered ground (Ref. 16), and extra ground attenuation (Ref. 17). The aircraft sources are then analytically "flown" through a trajectory (See Table 2, Ref. 13) and spectra are then calculated at half-second intervals using a code developed by Clark (Ref. 18).

Thermodynamic and geometric engine data are calculated for the core and jet noise models using the thermodynamic cycle analysis tool described in Reference 19. With a design bypass ratio of 13.5 and fan tip speed of only 850 ft/s, the low spool is very likely to be geared so that the low pressure turbine is limited to a reasonable diameter. Selected sea level static design point and certification condition properties for a 537 °R day are summarized in Table 3.

Results and Discussion

The tone-weighted perceived noise level variation around the airplane in pitch angle is shown in Figure 9. The data are shown both with and without wing barrier diffraction calculations. Shown in the first plot are the levels at a one thousand foot radius in a 200 knot free field for four fan noise sources. With the engine and wing geometry listed in Table 2, a maximum barrier attenuation of 14.2 PNdB occurs at a pitch angle of 140 degrees below and behind the wing. Shown in the sec-

ond plot is the noise level variation with all sources considered. With no barrier calculations applied to airframe and jet noise, the maximum shielding effect is reduced to only 9.2 PNdB at a pitch angle of 140 degrees. This limitation of the barrier effectiveness is a result of the low noise signature of the study engine relative to airframe noise and becomes important in the certification noise predictions described below.

The airplane is analytically flown through its trajectory as described earlier and noise histories are calculated for each certification observer. Sample noise histories are shown in Figure 10 for the community observer. Shown in the first plot are the histories without wing barrier diffraction calculations. As expected, the trace is dominated by fan discharge noise. The low specific thrust of the engine is evident from the extremely low levels of jet noise. Shown in the second plot are the histories when the wing barrier is considered. Also as expected, the wing effectively eliminates the fan discharge and core noise relative to the other unshielded noise sources. In the shielded case, fan inlet and airframe noise dominate the trace. Fan inlet noise is not shielded well for a flyover observer with the geometry considered. Fan discharge noise rises again later in the trace as the observer quickly emerges from the transition zone, but it does not contribute significantly to the effective perceived noise level. The unsteadiness seen in the traces is due mainly to irregularities in the spectra introduced by ground reflection calculations and accentuated by the tone penalty component of the noise metric. The noise histories for the other certification observers are similar and are not shown.

Effective perceived noise levels for the sideline, community, and approach observers are shown in Figures 11 through 13, respectively. Contributions of the individual noise sources and the effectiveness of the wing barrier are shown. 90 and 95 EPNdB contours around the runway are shown in Figure 14. Mounting the engines above the wing results in a reduction of the 95 EPNdB footprint from 0.96 to 0.57 square miles. In certification parlance, the airplane in this study is 44.5 cumulative EPNdB below Stage 3 regulations, 9.9 cumulative EPNdB of which may be attributed to wing barrier shielding. This compares favorably with the certification noise levels of current large quads, which are approximately 10 cumulative EPNdB below Stage 3 regulations (Ref. 13).

Conclusions

The noise of advanced turbofan engines is shown to be effectively shielded in an over-the-wing mounted installation. Making this possible is the dominance of the fan discharge noise and the relatively low levels of

distributed jet noise. Mounting the engines above the wing may also result in other forms of noise reduction not considered in this study. The enhancement of low frequency boundary layer noise due to the entrainment of air between the wing and the jet can often be substantial (Ref. 20). Mounting the engines above the wing would eliminate this additional noise source and would also prevent the wing from serving as a high frequency noise reflector. Although expensive, ground testing and in-flight measurements may be the only way to accurately measure shielding attenuation of a modern engine in a proper, full scale operating environment with realistic sources.

The low fan speed, low specific thrust engine considered here is remarkably quiet. Airframe noise is therefore predicted to become a significant noise source for the conceptual long haul quad aircraft studied. This conclusion is reached despite the airframe noise reduction levels assumed in this study, and it is especially true when the engine noise is reduced further via the wing shielding effect. Airframe noise has often been called the lower bound of certification noise, and it is certainly the case in this study. Airframe noise reductions are possible, however, and the airframe noise technologies assumed here may eventually need to be implemented on future aircraft.

References

1. Bloomer, H.: *Investigation of Wing Shielding Effects on CTOL Engine Noise*. AIAA 79-0669, 1979.
2. Neubert, R.; Bock, L.; Malmberg, E.; and Owen-Peer, W.: *Advanced Low Noise Research Fan Stage Design*. NASA CR 97-206308, 1997.
3. Kontos, K.; Janardan, B.; and Gliebe, P.: *Improved NASA-ANOPP Noise Prediction Computer Code for Advanced Subsonic Propulsion Systems. Volume 1: ANOPP Evaluation and Fan Noise Model Improvement*. NASA CR 195480, 1996.
4. Maekawa, Z.: *Noise Reduction by Screens*. Memoirs of the Faculty of Engineering, Kobe University, Japan, vol. 12, 1966, pp. 472-479.
5. Mitchell, J.; Barton, C.; Kisner, L.; and Lyon, C.: *Computer Program to Predict Noise Levels of General Aviation Aircraft: User's Guide*. NASA CR 168050, 1982.
6. Larson, R.; Robbins, K.: *Refraction of Sound by Aircraft Wingtip Vortices*. AIAA-80-0975, 1980.
7. Hellstrom, G.: *Noise Shielding Aircraft Configurations, A Comparison Between Predicted and Experimental Results*. ICAS Paper No. 74-58, 1974.
8. Low, K.: *Ultra-High Bypass Ratio Jet Noise*. NASA CR 195394, 1994.

9. *Proposed Coaxial Jet Noise Prediction Procedure*. Aerospace Recommended Practice 876, Rev. C, 1975, SAE.
10. Stone, J.: *An Improved Prediction Method for Noise Generated by Conventional Profile Coaxial Jets*. NASA TM 82712, 1981.
11. Emmerling, J.; Kazin, S.; and Matta, R.: *Core Engine Noise Control Program. Volume III, Supplement 1 - Prediction Methods*. FAA-RD-74-125, III-I, March 1976.
12. Fink, M.: *Airframe Noise Prediction Method*. FAA-RD-77-29, March, 1977.
13. Kumasaka, H.; Martinez, M.; and Weir, D.: *Definition of 1992 Technology Aircraft Noise Levels and the Methodology for Assessing Airplane Noise Impact of Component Noise Reduction Concepts*. NASA CR 198298, 1996.
14. *Standard Values of Atmospheric Absorption as a Function of Temperature and Humidity*. Aerospace Recommended Practice 866, 1964, SAE.
15. Putnam, T.: *Review of Aircraft Noise Propagation*. NASA TM-X-56033, 1975.
16. Delaney, M.; and Bazley, E.: *Acoustical Properties of Fibrous Absorbent Materials*. Applied Acoustics, Vol 3, No 2, Apr 1970, pp 105-116.
17. *Method for Calculating the Attenuation of Aircraft Ground to Ground Noise Propagation during Takeoff and Landing*. Aerospace Information Report 923, Aug. 15, 1966, SAE.
18. Clark, B.: *Computer Program to Predict Aircraft Noise Levels*. NASA TP 1913, 1981.
19. Klann, J.; and Snyder, C.: *NEPP Programmers Manual, Volume I: Technical Description*. NASA TM 106575, 1994.
20. Wang, M.: *Wing Effect on Jet Noise Propagation*. AIAA Paper No. 80-1047, 1980.

Parameter	Value
Wing semispan ($b/2$, ft)	100
Root chord (c_0 , ft)	43
Tip chord (c_t , ft)	13
Leading edge sweep (Λ_{LE} , deg)	35
Inboard engine location (y_{EIB} , ft)	41
Outboard engine location (y_{EOB} , ft)	68
Nacelle length (L_E , in)	198
Engine height above wing (h_E , in)	90
Inlet to leading edge (f_E , in)	132

Table 1: Dimensions for the baseline aircraft configuration of Figure 5

Flight Condition	Altitude (ft)	True Airspeed (kts)	Climb Angle (deg)	Engine Pitch (deg)
Approach	394	175	-3	3
Sideline	1000	205	7	17
Community	1100	205	2	12

Table 2: Takeoff and landing reference trajectory data for a large quad aircraft

	Sea Level, Static Design Point	Sideline (1000 ft/205 kts)	Community (1100 ft/205 kts)	Approach (394 ft/175 kts)
Corrected airflow (lb/s)	2664	2919	2607	1665
Fan pressure ratio	1.284	1.280	1.212	1.069
Overall pressure ratio	38.3	37.8	30.2	13.6
Combustor entrance total temperature (°R)	1628	1632	1529	1234
Combustor entrance total pressure (psia)	547	557	442	202
Combustor exit total temperature (°R)	3260	3260	2977	2187
Turbine rotor inlet total temperature (°R)	3083	3083	2818	2080
Primary jet velocity (ft/s)	1110	1156	926	426
Primary jet total temperature (°R)	1465	1456	1357	1140
Primary nozzle pressure ratio	1.288	1.319	1.207	1.048
Secondary jet velocity (ft/s)	666	752	675	424
Secondary jet total temperature (°R)	584	587	577	554
Secondary nozzle pressure ratio	1.259	1.342	1.271	1.102
Gross thrust (lb)	57300	70200	55600	21800
Net thrust (lb)	57300	38600	27500	6400

Table 3: Engine cycle data

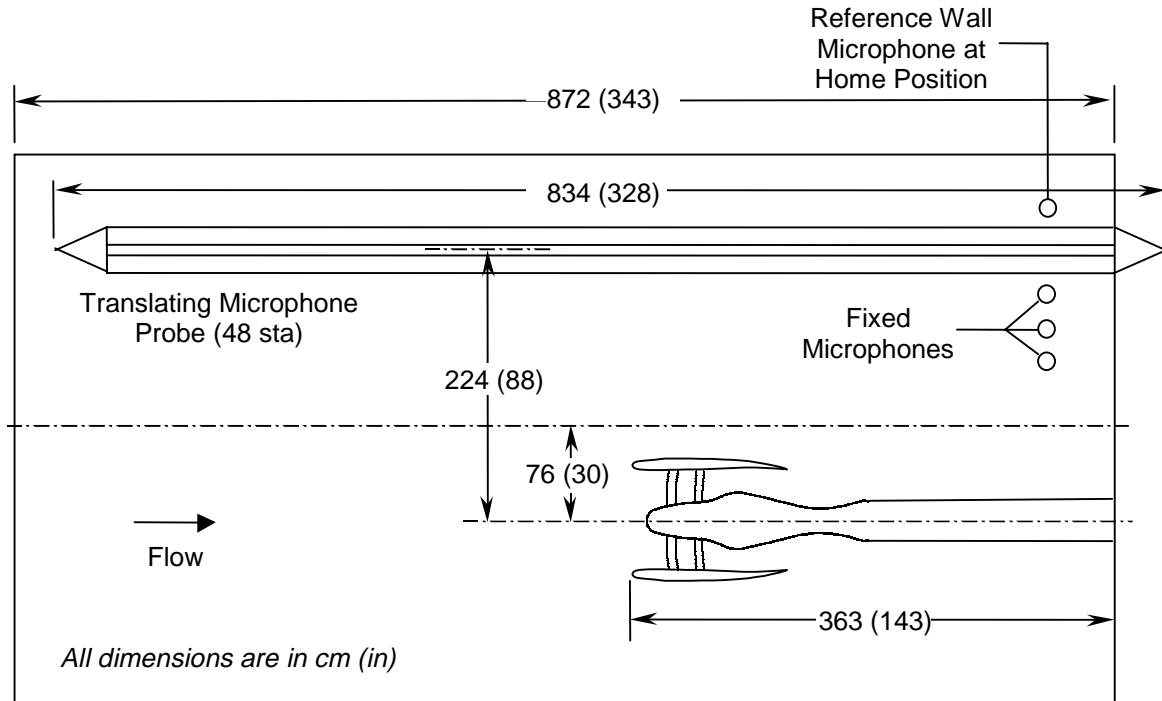


Figure 1: Fan rig in NASA Glenn 9x15 Low Speed Wind Tunnel

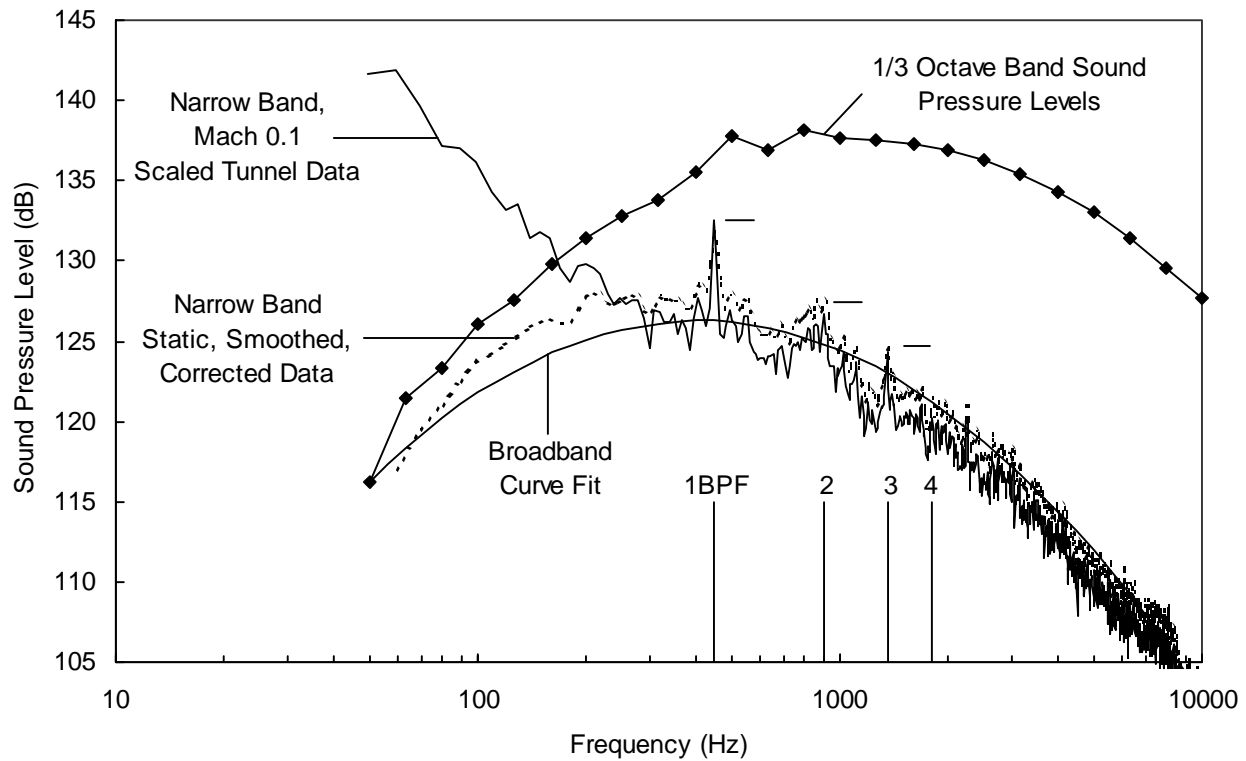


Figure 2: Experimental fan noise data reduction

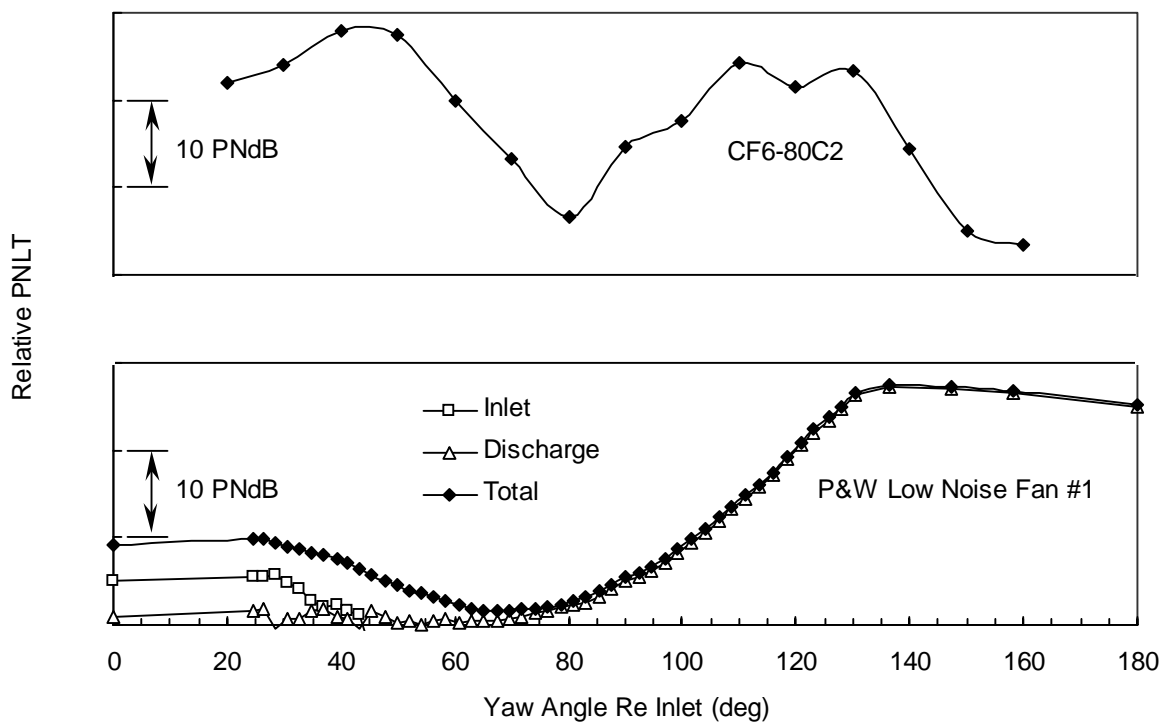


Figure 3: Static fan noise comparison

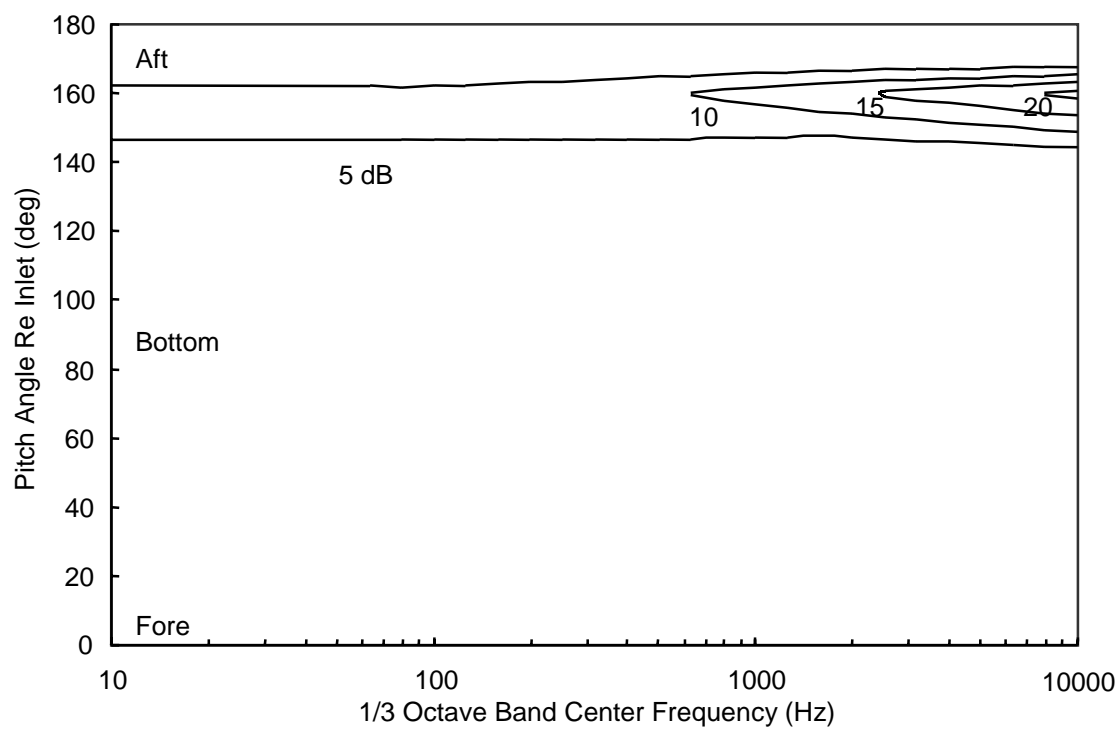


Figure 6: Inlet barrier attenuation

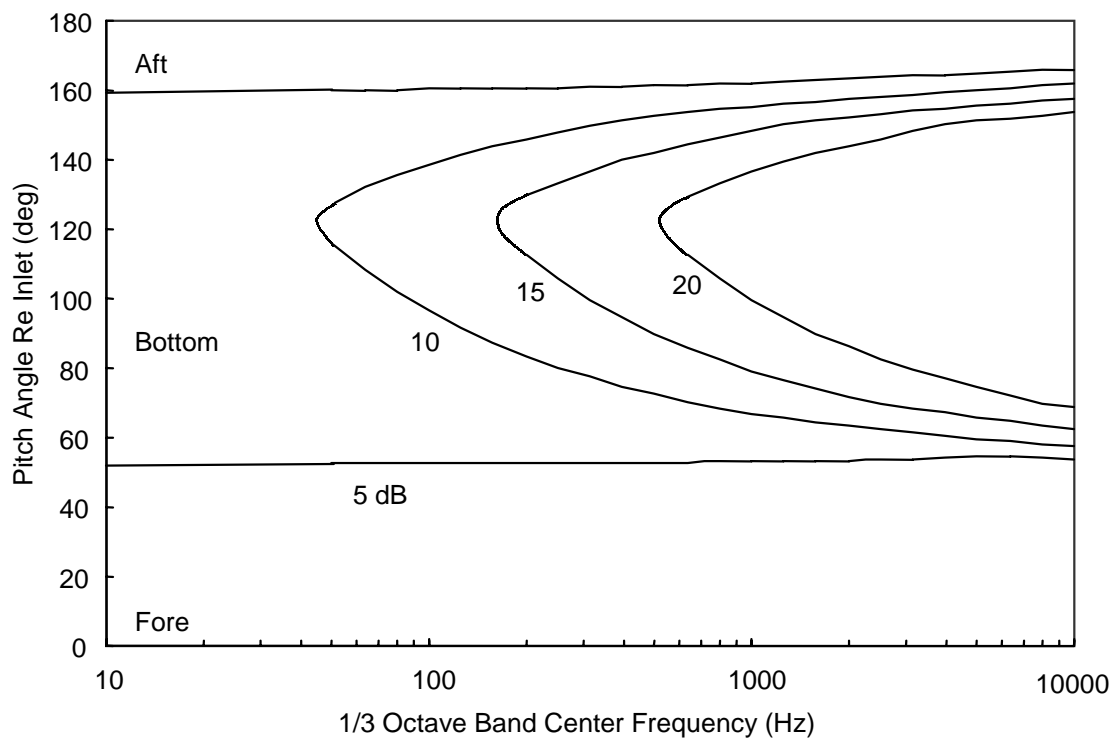


Figure 7: Discharge barrier attenuation

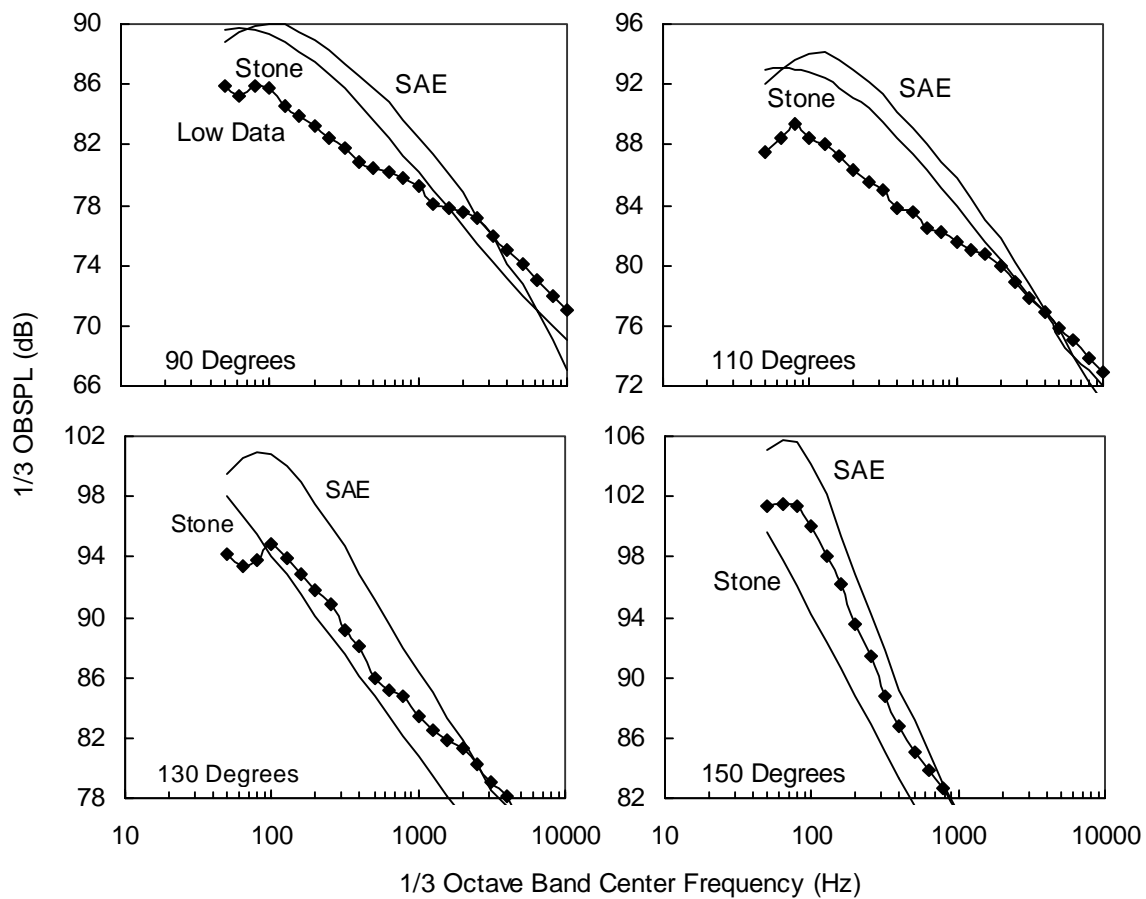


Figure 8: Jet noise modeling

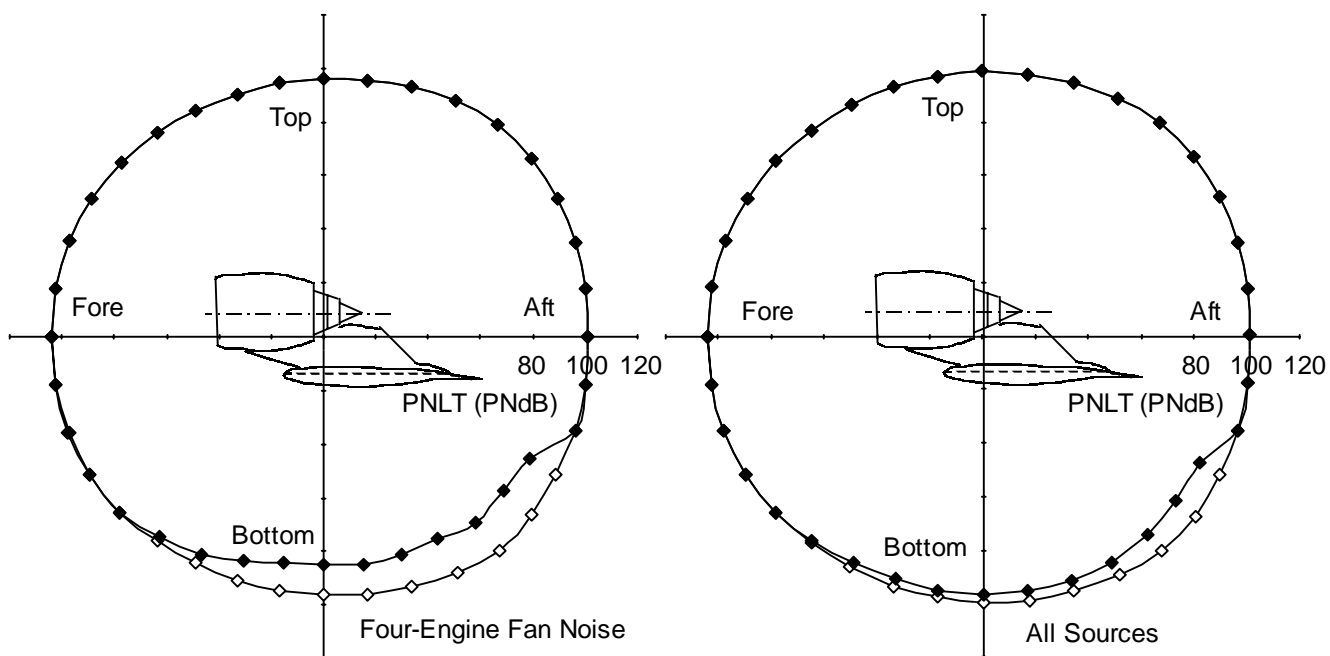


Figure 9: Noise level variation in pitch angle; with and without wing barrier diffraction calculations

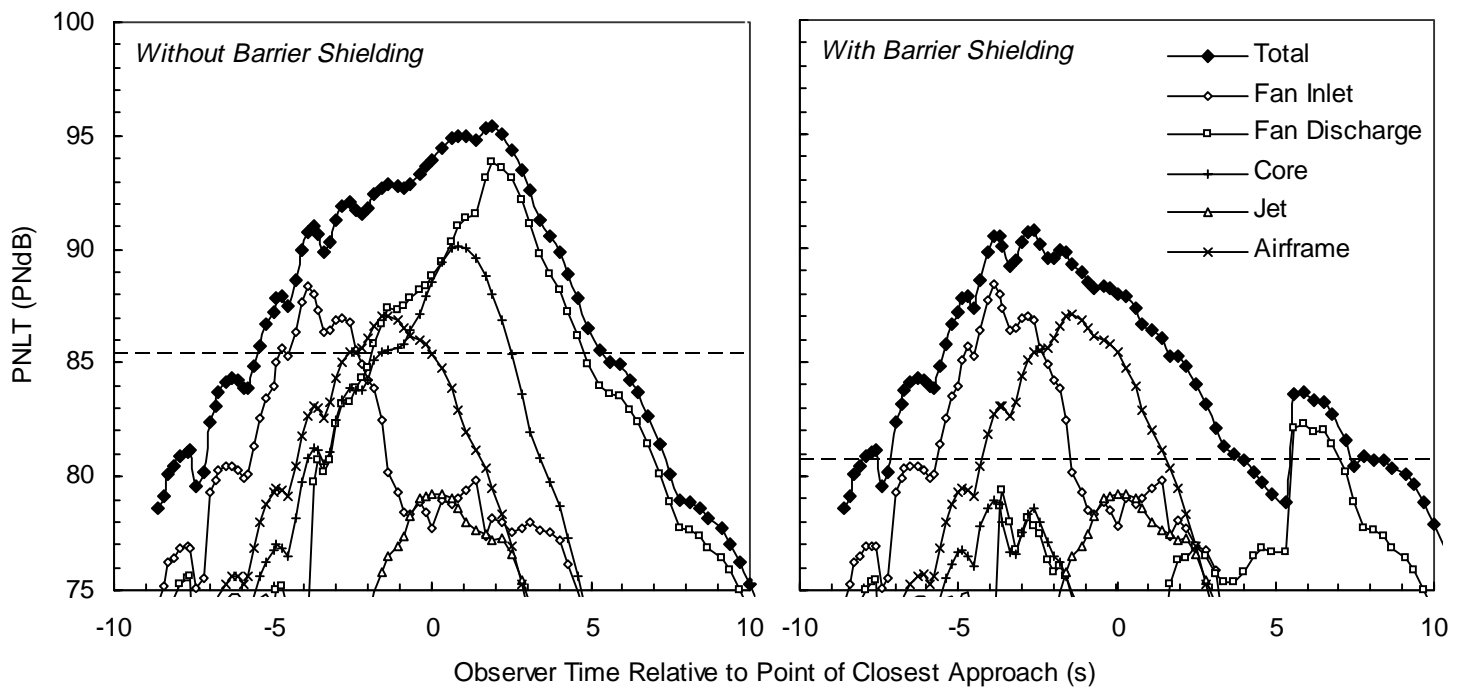


Figure 10: Community observer noise histories, with and without wing barrier diffraction calculations

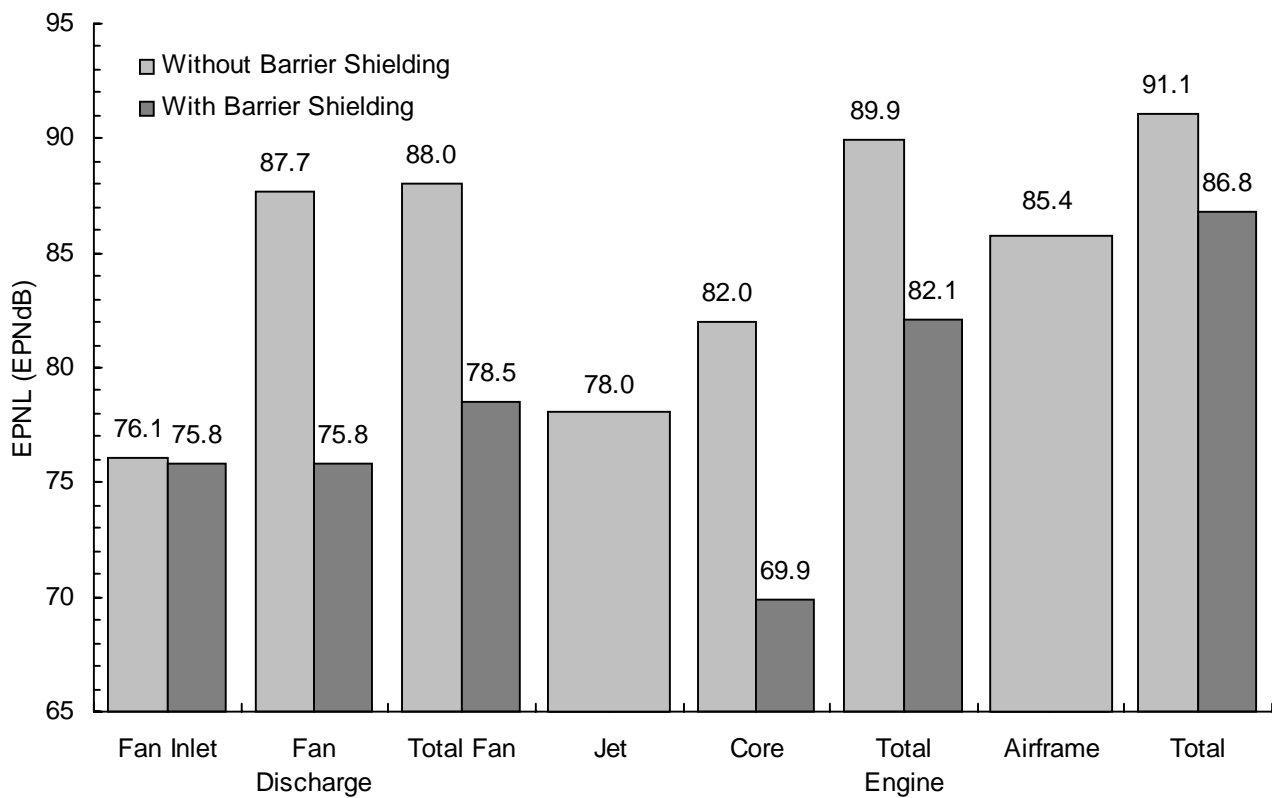


Figure 11: Sideline noise prediction, showing influence of wing barrier calculations

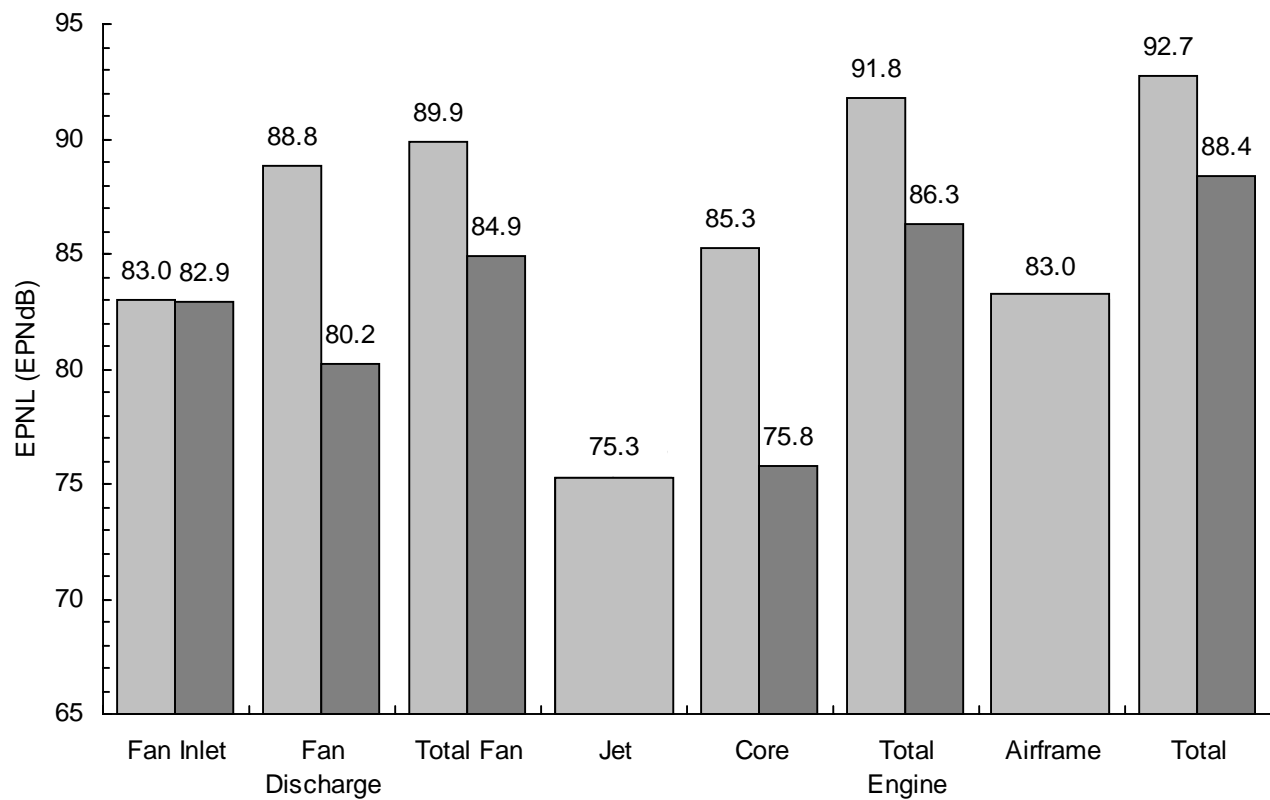


Figure 12: Community noise prediction, showing influence of wing barrier calculations

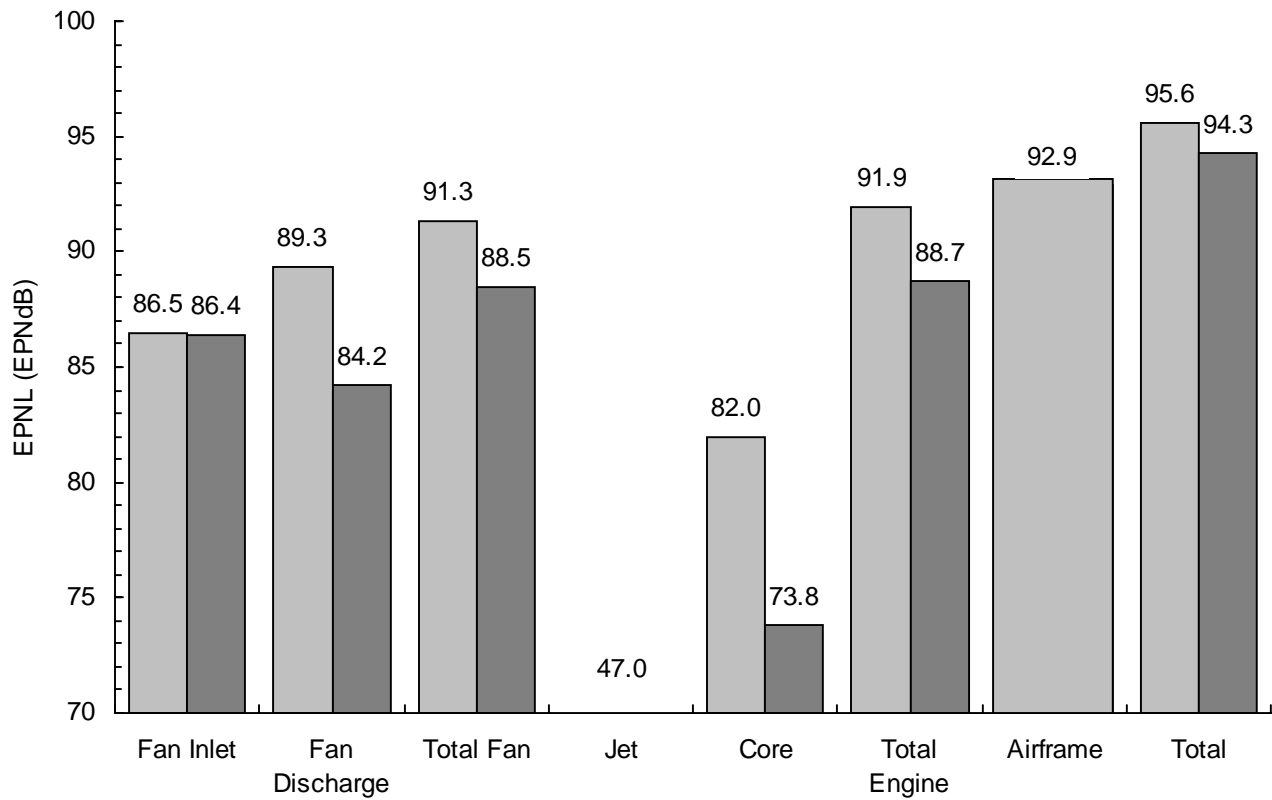


Figure 13: Approach noise prediction, showing influence of wing barrier calculations

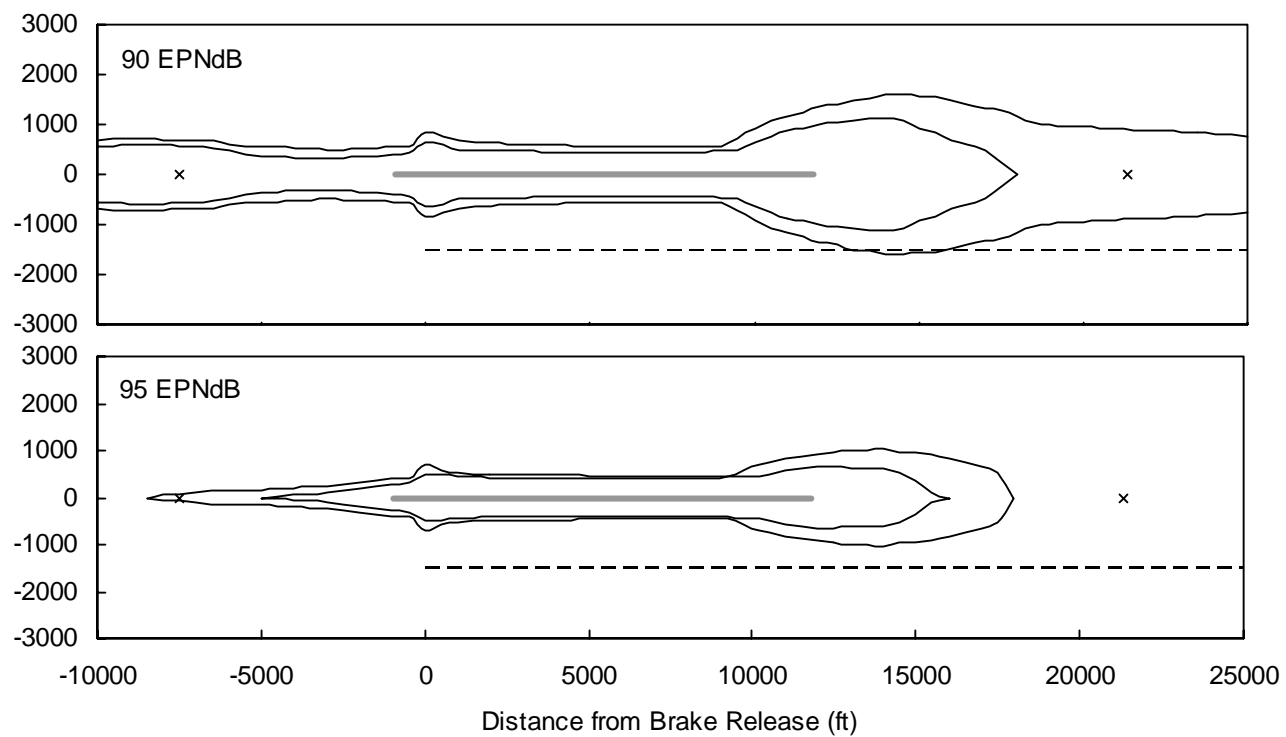


Figure 14: Plan view of runway with 90 and 95 EPNdB contours, showing influence of wing barrier calculations

REPORT DOCUMENTATION PAGE			Form Approved OMB No. 0704-0188	
Public reporting burden for this collection of information is estimated to average 1 hour per response, including the time for reviewing instructions, searching existing data sources, gathering and maintaining the data needed, and completing and reviewing the collection of information. Send comments regarding this burden estimate or any other aspect of this collection of information, including suggestions for reducing this burden, to Washington Headquarters Services, Directorate for Information Operations and Reports, 1215 Jefferson Davis Highway, Suite 1204, Arlington, VA 22202-4302, and to the Office of Management and Budget, Paperwork Reduction Project (0704-0188), Washington, DC 20503.				
1. AGENCY USE ONLY (Leave blank)	2. REPORT DATE April 2000	3. REPORT TYPE AND DATES COVERED Technical Memorandum		
4. TITLE AND SUBTITLE Noise Reduction Potential of Large, Over-the-Wing Mounted, Advanced Turbofan Engines		5. FUNDING NUMBERS WU-714-99-20-00		
6. AUTHOR(S) Jeffrey J. Berton				
7. PERFORMING ORGANIZATION NAME(S) AND ADDRESS(ES) National Aeronautics and Space Administration John H. Glenn Research Center at Lewis Field Cleveland, Ohio 44135-3191		8. PERFORMING ORGANIZATION REPORT NUMBER E-12222		
9. SPONSORING/MONITORING AGENCY NAME(S) AND ADDRESS(ES) National Aeronautics and Space Administration Washington, DC 20546-0001		10. SPONSORING/MONITORING AGENCY REPORT NUMBER NASA TM-2000-210025		
11. SUPPLEMENTARY NOTES Prepared for the 14th International Symposium on Air Breathing Engines sponsored by the International Society for Air Breathing Engines, Florence, Italy, September 5-10, 1999. Responsible person, Jeffrey J. Berton, organization code 2400, (216) 977-7031.				
12a. DISTRIBUTION/AVAILABILITY STATEMENT Unclassified - Unlimited Subject Category: 07 This publication is available from the NASA Center for AeroSpace Information, (301) 621-0390.			12b. DISTRIBUTION CODE	
13. ABSTRACT (Maximum 200 words) As we look to the future, increasingly stringent civilian aviation noise regulations will require the design and manufacture of extremely quiet commercial aircraft. Indeed, the noise goal for NASA's Aeronautics Enterprise calls for technologies that will help to provide a 20 EPNdB reduction relative to today's levels by the year 2022. Further, the large fan diameters of modern, increasingly higher bypass ratio engines pose a significant packaging and aircraft installation challenge. One design approach that addresses both of these challenges is to mount the engines above the wing. In addition to allowing the performance trend towards large, ultra high bypass ratio cycles to continue, this over-the-wing design is believed to offer noise shielding benefits to observers on the ground. This paper describes the analytical certification noise predictions of a notional, long haul, commercial quadjet transport with advanced, high bypass engines mounted above the wing.				
14. SUBJECT TERMS Noise prediction (aircraft); Aircraft noise; Jet aircraft noise			15. NUMBER OF PAGES 19	
			16. PRICE CODE A03	
17. SECURITY CLASSIFICATION OF REPORT Unclassified	18. SECURITY CLASSIFICATION OF THIS PAGE Unclassified	19. SECURITY CLASSIFICATION OF ABSTRACT Unclassified	20. LIMITATION OF ABSTRACT	